Experimental and theoretical evidence for the existence of photonic bandgaps and selective transmissions in serial loop structures

E. El Boudouti, N. Fettouhi, Abdellatif Akjouj, Bahram Djafari-Rouhani, A. Mir, J. Vasseur, Jerome O. Vasseur, L. Dobrzynski, J. Zemmouri

Experimental and theoretical evidence for the existence of photonic bandgaps and selective transmissions in serial loop structures

Cite as: Journal of Applied Physics **95**, 1102 (2004); https://doi.org/10.1063/1.1633983
Submitted: 22 July 2003 • Accepted: 27 October 2003 • Published Online: 20 January 2004

E. H. El Boudouti, N. Fettouhi, A. Akjouj, et al.

Experimental and theoretical evidence for the existence of photonic bandgaps and selective transmissions in serial loop structures

E. H. El Boudouti
Laboratoire de Dynamique et d'Optique des Matériaux, Département de Physique, Faculté des Sciences, Université Mohamed I, 60000 Oujda, Morocco

N. Fettouhi
Département de Physique, Faculté des Sciences, Université Moulay Ismail, Meknès, Morocco

A. Akjouj[a] and B. Djafari-Rouhani
EDI, UMR CNRS 8024, UFR de Physique, Université de Lille I, 59655 Villeneuve d'Ascq, France

A. Mir
Département de Physique, Faculté des Sciences, Université Moulay Ismail, Meknès, Morocco

J. O. Vasseur and L. Dobrzynski
EDI, UMR CNRS 8024, UFR de Physique, Université de Lille I, 59655 Villeneuve d'Ascq, France

J. Zemmouri
PHLAM, UMR CNRS 8523, UFR de Physique, Université de Lille I, 59655 Villeneuve d'Ascq, France

(Received 22 July 2003; accepted 27 October 2003)

We have investigated the electromagnetic band structure, transmission, and phase time through a one-dimensional structure made of loops pasted together with segments of finite length. In this serial loop structure, the loops and segments are constituted of dielectric monomode materials. Analytic expressions are reported for the band structure for a large number N of loops and for transmission coefficients and phase times for any value of N. Experimental and numerical results show the existence of large gaps in these structures. These gaps originate both from the periodicity of the system and the loop resonant states that create zeroes of transmission. The gap widths depend on the lengths of the finite segment and the loop diameters. Defect modes may occur in these bandgaps by introducing defective segments in the structure. The localized states appear as very narrow peaks both in the transmission spectrum and in the transmission phase time of finite serial loop structures. The localized state behavior is analyzed as a function of the length and of the position of the defect segment. The transmission phase measurements enable us to derive the group velocity as well as the density of states in these structures. The experimental results are obtained using coaxial cables in the frequency range of few hundreds of MHz. © *2004 American Institute of Physics.*
[DOI: 10.1063/1.1633983]

I. INTRODUCTION

Photon propagation in artificial periodic dielectric structures may give rise to photonic bandgaps (PBGs),[1,2] where electromagnetic modes, spontaneous emission, and zero-point fluctuations are all prohibited.[3,4] These PBGs are analogs, for electrons, to the electronic bandgaps in the band structure of semiconductor crystals. Of particular interest is the existence of PBG in the band structure of one-dimensional (1D) structures with a variety of geometries.[5–9] In previous papers,[7,8] we demonstrated that the electromagnetic transmission spectrum of quasi-1D comb structures exhibits large gaps. These structures, called *star waveguides*, are composed of an infinite backbone along which stars of N' finite branches are grafted at N equidistant sites, N and N' being integers. The stop bands originate from the periodicity of the system determined by the distance between two neighboring sites and from the eigenmodes of the dangling side branches that play the role of resonators. The gap widths depend also on the boundary conditions at the free ends of the side branches; namely, the vanishing of either the electric field ($E=0$) or the magnetic field ($B=0$). In such systems, the propagation is monomode, provided the two characteristic lengths (the periodicity and the resonator length) and the wavelength are much larger than the backbone and the side branch diameters.[7,8] It is worthwhile to point out that this star waveguide exhibits relatively broad forbidden bands even if the backbone and the resonators are made of the same material;[7] in other words, the existence of the gaps does not require a contrast between the parameters of the two constituents. This property offers the possibility of engineering bandgaps in homogeneous materials. Moreover localized modes may appear in the forbidden bands when a defect is introduced in the star waveguide periodic structure. Applications such as selective frequency filters and efficient waveguides[9] may be expected.

In a recent work, Zhang *et al.*[10] studied theoretically and experimentally three-dimensional PBG systems constructed by segments and loops made of coaxial cables arranged in a

[a]Electronic mail: abdellatif.akjouj@univ-lille1.fr

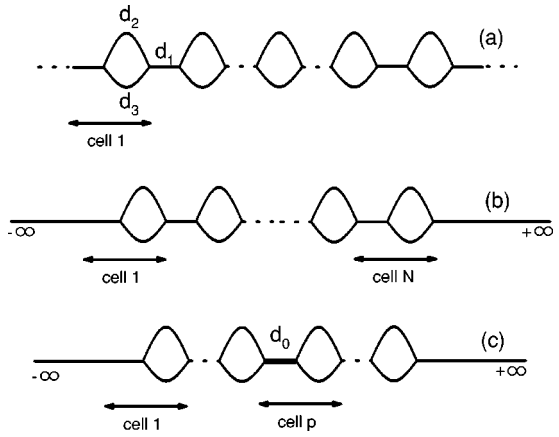

FIG. 1. (a) Schematic of the 1D serial loop structures studied in this work. The media are labeled by an index i, with $i=1$ for the finite branch and 2 and 3 for the loop. Each loop has a length d_2+d_3 and is distant by d_1 from the neighboring loops. Each cell is composed of a finite branch and the loop connected to its right. (b) Waveguide with finite N loops separated by a length d_1 and connected at its extremities to two semi-infinite leading lines. (c) Same as in (b), except that a defect branch of length d_0 (heavy line) is introduced in the cell p.

diamond structure. The transmission measurement shows a wide gap, but the presence of the free ends of the structure induces a surface state, which makes the gap not truly forbidden for all states. In addition, besides the Anderson localized state observed in random structures, defect modes are introduced in the gap by changing the length of one loop in an ordered network. However, the peak associated with the defect mode is not well defined because of the dissipation inside the cables. In this article, we study a 1D structure made of segments and loops, called it *serial loop structure* (SLS) exhibiting large gaps, and in which the existence of defect modes can be clearly observed. This SLS may be modeled as an infinite number of unit cells pasted together. Each cell is made of a finite segment of length d_1 connected to a loop of length d_2+d_3 [each loop is composed of two wires of different lengths $d_2 \neq d_3$, see Fig. 1(a)]. The propagation of electromagnetic waves through SLSs is also assumed to be monomode. The simple analytical expressions obtained enables us to explain clearly the origin of the band gaps as a function of the different lengths of segments and loops. Indeed, the SLS allows us to distinguish two different structures: (i) the symmetric SLS (i.e., $d_2=d_3$), in which the band gaps result only from the periodicity $d=d_1+d_2$ of the SLS and (ii) the asymmetric SLS (i.e., $d_2 \neq d_3$), in which the bandgaps result from both the periodicity and the transmission zeroes in these systems. In particular the phase time measurements show different behaviors in these two cases, in accordance with recent experiments on phase-coherent transport through a quantum dot.[11,12] The phase time measurements also enable us to determine the group velocity, which can exceed the speed of light in vacuum or even become negative. The existence of such phenomena has attracted much attention in the last few years,[13–15] with the challenge to attain a pulse advancement comparable to the pulse width with a low level of pulse distortion. The SLS may also show additional features in comparison with star waveguides, such as the existence of larger gaps and the absence of the boundary condition at the end of the side branches, which could be of potential interest in optical waveguide structures. These features are essentially due to the loop structure, which is quite different from the case of a simple resonator.[7,8] The introduction of defects inside the SLS structure may give rise to well-defined defect modes inside the band gaps in the transmission spectra.

The experimental demonstration of our theoretical predictions is performed by measuring the transmission spectra through finite SLS constituted by coaxial cables. The typical length of the cables is on the order of a meter, and, therefore, the frequencies fall in the range of 10 to 500 MHz. Let us mention that, besides our previous papers,[7,8] recent work also dealt with photonic circuits constituted by an alternative repetition of two different coaxial cables,[16,17] indicating that the behaviors observed in these 1D crystals are qualitatively comparable to those of photonic systems of higher dimension as well.

The theoretical model developed here falls within the framework of the interface response theory of continuous media,[18] which we recall briefly in Sec. II. The analytical expressions for the band structure of an infinite SLS and for the transmission coefficient of a finite SLS with and without a defect are given in Sec. III. Section IV is devoted to a numerical discussion of these expressions. The theoretical predictions are then compared to experimental measurements of the electromagnetic transmission spectra through a finite SLS composed of standard coaxial cables. Finally, some conclusions are drawn in Sec. V.

II. THEORETICAL MODEL

A. Interface response theory of continuous media

Our theoretical analysis is performed with the help of the interface response theory of continuous media, which allows to calculate the Green's function of any composite material. In what follows, we present the basic concept and the fundamental equations of this theory.[18]

Let us consider any composite material contained in its space of definition D and formed out of N different homogeneous pieces situated in their domains D_i. Each piece is bounded by an interface M_i, adjacent in general to j $(1 \leqslant j \leqslant J)$ other pieces through subinterface domains M_{ij}. The ensemble of all these interface spaces M_i will be called the interface space M of the composite material.

The elements of the Green's function $g(DD)$ of any composite material can be obtained from[18]

$$g(DD)=G(DD)-G(DM)G^{-1}(MM)G(MD) + G(DM)G^{-1}(MM)g(MM)G^{-1} \times G^{-1}(MM)G(MD), \quad (1)$$

where $G(DD)$ is the reference Green's function formed out of truncated pieces in D_i of the bulk Green's functions of the infinite continuous media and $g(MM)$, the interface element of the Green's function of the composite system.

The knowledge of the inverse of $g(MM)$ is sufficient to calculate the interface states of a composite system through the relation[18]

$$\det[g^{-1}(MM)]=0. \tag{2}$$

Moreover, if $U(D)$ represents an eigenvector of the reference system, Eq. (1) enables the calculation of the eigenvectors $u(D)$ of the composite material, and

$$u(D)=U(D)-U(M)G^{-1}(MM)G(MD) + U(M)G^{-1}(MM)g(MM)G^{-1}(MM)G(MD). \tag{3}$$

In Eq. (3), $U(D)$, $U(M)$, and $u(D)$ are row vectors. Equation (3) provides a description of all the waves reflected and transmitted by the interfaces, as well as the reflection and transmission coefficients of the composite system. In this case, $U(D)$ is a bulk wave launched in one homogeneous piece of the composite material.[19]

B. Inverse surface Green's functions of the elementary constituents

We consider an infinite homogeneous isotropic dielectric wire i characterized by its characteristic impedance z_i. The Fourier transformed Green's function between two points x and x' of this wire is[20]

$$G_i(x,x')=-\frac{e^{-\alpha_i|x-x'|}}{2F_i}, \tag{4}$$

where

$$\alpha_i=-j\frac{\omega}{c}\sqrt{\varepsilon_i(\omega)}, \tag{5a}$$

and

$$F_i=-\frac{1}{z_i}=\alpha_i, \tag{5b}$$

where $\varepsilon_i(\omega)$ is the relative permittivity, ω the angular frequency of the wave, c the speed of light in vacuum, F_i the admittance, and $j=\sqrt{-1}$.

Before addressing the problem of SLS, it is helpful to know the surface elements of the Green's function of a finite wire of length d_i and of a semi-infinite wire. The finite wire is bounded by two free surfaces located at $x=-d_i/2$ and $x=+d_i/2$. These surface elements can be written in the form of a (2×2) matrix $g_i(MM)$, within the interface space $M_i\equiv\{-d_i/2,+d_i/2\}$. The inverse of this matrix takes the following form:[20]

$$[g_i(MM)]^{-1}=\begin{pmatrix} -\frac{F_iC_i}{S_i} & \frac{F_i}{S_i} \\ \frac{F_i}{S_i} & -\frac{F_iC_i}{S_i} \end{pmatrix}, \tag{6a}$$

where $C_i=\cosh(\alpha_i d_i)$ and $S_i=\sinh(\alpha_i d_i)$. The inverse of the surface element of the Green's function of a semi-infinite wire is given by[20]

$$[g_i(00)]^{-1}=-F_i. \tag{6b}$$

III. DISPERSION RELATIONS AND TRANSMISSION COEFFICIENTS

The 1D serial loop waveguide can be considered as an infinite number of unit cells pasted together [see Fig. 1(a)]. Each cell is composed of a finite wire (medium *1*) of length d_1 in the direction x, connected to a loop "ring" (medium *2*) of length d_2+d_3 (each loop is constructed of two wires of lengths d_2 and d_3, respectively). The interface domain is made of all the connection points between finite segments and loops. A space position along the x axis in medium i belonging to the unit cell n is indicated by (n,i,x), where n (the "cell number") is an integer such that $-\infty\leqslant n\leqslant+\infty$, i is the medium index $(i=1,2,3)$, and $-d_i/2\leqslant x\leqslant+d_i/2$. Due to the 1D spatial periodicity of the system in the direction x, one can define a Bloch wave vector k along the axis of the waveguide.

Within the total interface space of the infinite SLS, the inverse of the matrix giving all the interface elements of the Green's function g is an infinite tridiagonal matrix formed by linear superposition of the elements $[g_i(MM)]^{-1}$ [Eq. (6)]. The explicit expression of the Green's function elements in the interface space is given as[21]

$$g(n,1,+d_1/2;n',1,+d_1/2) = g(n,1,-d_1/2;n',1,-d_1/2)=Y_1\frac{t^{|n-n'|+1}}{t^2-1}, \tag{7a}$$

$$g(n,1,+d_1/2;n',1,-d_1/2) = \frac{S_2S_3}{F_2S_3+F_3S_2}\frac{t^{|n-n'|+1}}{t^2-1}+\frac{S_1}{F_1}\frac{t^{|n-n'+1|+1}}{t^2-1}, \tag{7b}$$

$$g(n,1,-d_1/2;n',1,+d_1/2) = \frac{S_2S_3}{F_2S_3+F_3S_2}\frac{t^{|n-n'|+1}}{t^2-1}+\frac{S_1}{F_1}\frac{t^{|n-n'-1|+1}}{t^2-1}, \tag{7c}$$

where the integers n and n' refer to the cell number $(-\infty<n,n'<+\infty)$, and

$$Y_1=\frac{C_1S_2S_3+\frac{S_1}{F_1}(F_2C_2S_3+F_3C_3S_2)}{F_2S_3+F_3S_2}. \tag{8}$$

The parameter t is defined by

$$t=e^{jkd}, \tag{9}$$

and d is the period of the structure.

The dispersion relation of the infinite serial loop waveguide is obtained from Eq. (2). The stop bands are determined by the condition $|\xi|>1$, whereas the allowed bands are given by the condition $|\xi|<1$, where

$$\xi=\cos(kd)=\frac{1}{F_2S_3+F_3S_2}\left\{S_1S_2S_3\left(\frac{F_1^2+F_2^2+F_3^2}{2F_1}\right) + F_2C_1C_2S_3+F_3C_1C_3S_2+\frac{F_2F_3}{F_1}S_1(C_2C_3-1)\right\}. \tag{10}$$

The bandgaps of the structure may be also obtained from the transmission coefficient through a finite-sized serial loop structure. The finite SLS containing N equidistant loops is cut out of the infinite periodic system illustrated in Fig. 1(a) and this piece is subsequently connected at its extremities $[(1,1,+d_1/2),(N+1,1,-d_1/2)]$ to two semi-infinite leading lines [Fig. 1(b)]. An incident bulk electromagnetic wave $e^{-\alpha_s x}$ of unit amplitude launched from $x=-\infty$ is scattered by the interfaces between the dissimilar wires constituting the system. The index s refers to the semi-infinite media bounding SLS. The transmission function is then obtained with the help of Eqs. (3), (4), and (7) as

$$t_r=\frac{2F_sB(N)}{[A(N)-F_s]^2-B^2(N)}, \tag{11}$$

where $A(N)$ and $B(N)$ are given by

$$A(N)=\frac{Y_1Y_3-t^{2N-2}Y_2Y_4}{Y_1^2-t^{2N-2}Y_2^2}, \tag{12}$$

and

$$B(N)=\frac{Y_1Y_4-Y_2Y_3}{Y_1^2-t^{2N-2}Y_2^2}t^{N-1}, \tag{13}$$

where

$$Y_2=\frac{S_2S_3}{F_2S_3+F_3S_2}t+\frac{S_1}{F_1}, \tag{14}$$

$$Y_3=-\frac{1}{t}+\frac{F_2C_1C_2S_3+F_3C_1C_3S_2+F_1S_1S_2S_3}{F_2S_3+F_3S_2}, \tag{15}$$

and

$$Y_4=C_1-\frac{F_2C_2S_3+F_3C_3S_2}{F_2S_3+F_3S_2}t. \tag{16}$$

The transmission function can be written in an explicit complex form as

$$t_r=a+jb=\sqrt{T}e^{j\varphi} \tag{17}$$

where T is the transmission coefficient and $\varphi=\arctan(b/a)\pm l\pi$ is the phase associated with the transmission field and l is an integer. The first derivative of φ with respect to the frequency is indicative of the delay time taken by the wave to go through the structure. This quantity, called phase time, is defined by[22–26]

$$\tau=\frac{d\varphi}{d\omega}. \tag{18}$$

On the other hand, a defect can be created in the SLS by replacing a segment d_1 in the cell $(n=p)$ by a segment of different length $d_0\neq d_1$ [Fig. 1(c)]. Within the Green's function formalism, one can calculate analytically the corresponding localized state frequencies. Theses frequencies satisfy the equation

$$\left\{1+\frac{t}{t^2-1}(Y_1-Y_5)\left[\frac{-F_0(C_0+1)}{S_0}+\frac{F_1(C_1+1)}{S_1}\right]\right\}\times\left\{1+\frac{t}{t^2-1}(Y_1+Y_5)\left[\frac{-F_0(C_0-1)}{S_0}+\frac{F_1(C_1-1)}{S_1}\right]\right\}=0, \tag{19}$$

where the index 0 refers to the defect segment and

$$Y_5=\frac{S_2S_3}{F_2S_3+F_3S_2}+\frac{S_1}{F_1}t. \tag{20}$$

The transmission function through a defective SLS with a finite number N of cells and containing a defect located in the cell p $(1<p\leqslant N)$ can be obtained as

$$t_r'=\frac{2F_s(F_0/S_0)B(N)B(p)}{Y(N)Y(p)-(F_0/S_0)^2(A(N)-F_s)(A(p)-F_s)}, \tag{21}$$

where $Y(q)$ is given by

$$Y(q)=B^2(q)-[A(q)-F_1]\left[A(q)-\frac{F_0C_0}{S_0}\right], \tag{22}$$

with $q\equiv N$ or p. The other parameters in Eq. (22) were given earlier.

From the previous general equations, one can deduce two particular cases corresponding to specific lengths of the loop.

(i) The tangent SLS, which corresponds to $d_2\neq 0$ and $d_3=0$. In this case, ξ [Eq. 10)] becomes

$$\xi=C_1+\frac{F_2}{F_1}\frac{S_1S_2'}{C_2'}, \tag{23}$$

where $S_2'=\sinh(\alpha_2d_2/2)$ and $C_2'=\cosh(\alpha_2d_2/2)$. This relation is equivalent to the dispersion relation of a star waveguide along which two resonators of length $d_2/2$ are grafted periodically. This system was largely investigated both theoretically and experimentally.[7,8] The forbidden bands in the dispersion curves result from the periodicity of the structure as well as the zeroes of transmission due to the resonators.

(ii) A symmetric SLS characterized by identical arms of the loop (i.e., $d_2=d_3$). In this case, the dispersion relation becomes

$$\xi=C_1C_2+\frac{1}{2}\left(\frac{F_1}{2F_2}+\frac{2F_2}{F_1}\right)S_1S_2. \tag{24}$$

This relation is analogous to the dispersion relation of a superlattice constituted out of two different layers.[27,28] The two layers should be of lengths d_1 and d_2 and characterized by their admittances F_1 and $2F_2$, respectively. The bandgaps result only from the periodicity of the system. Several theoretical studies have dealt in the past with electromagnetic waves in superlattices with defects.[29–32] The experimental evidence of the existence of defect modes in 1D photonic crystals constructed by connecting segments of coaxial cables of different characteristic impedances was presented recently by Schneider *et al.*[16] However,

in all these studies, the contrast between the dielectric constants in the two constituting layers is a critical parameter for the stop band to exist. In this work, we show that symmetric SLS may exhibit large gaps and defect modes even if the loops and the segments are made of the same materials, which could be of potential interest in optical waveguide structures.

In the next section, we shall show the origin of the gaps in SLSs as well as the evolution of the bandgap structure when the lengths of the wires constituting the SLS vary between the two limiting cases (i) and (ii) just mentioned.

IV. NUMERICAL AND EXPERIMENTAL RESULTS

A. A single loop

Before illustrating these analytical results by numerical calculations confirmed experimentally with coaxial cables, let us consider the elementary case of a waveguide consisting of a single loop. From Eq. (11), one can derive the analytical expression of the transmission coefficient of a single homogeneous loop by setting $N=1$. For the sake of simplicity, we have limited ourselves to the case in which the media constituting the SLS are made of identical materials (i.e., $z_1=z_2=z_3$ and $\varepsilon_1=\varepsilon_2=\varepsilon_3=\varepsilon$). The transmission coefficient is shown to be

$$T=\left|\frac{2(S_2+S_3)S_2S_3}{(C_2S_3+C_3S_2+S_2S_3)^2-(S_2+S_3)^2}\right|^2. \tag{25}$$

This coefficient equals zero only when $S_2+S_3=0$, or equivalently, $2\sin(\alpha' L/2)\cos(\alpha'\Delta L/2)=0$, where $\Delta L=d_2-d_3$, $L=d_2+d_3$, and $\alpha'=\omega\sqrt{\varepsilon}/c$. Therefore, zeroes of transmission occur at frequencies such that $\alpha' L=2m\pi$ and $\alpha'\Delta L=(2m'+1)\pi$, or equivalently,

$$f_m=\frac{c}{\sqrt{\varepsilon}}\left(m+\frac{1}{2}\right)\frac{1}{\Delta L}, \tag{26}$$

and

$$f_{m'}=\frac{c}{\sqrt{\varepsilon}}\frac{m'}{L}, \tag{27}$$

where m and m' are integers.

It is worth noticing that for frequencies given by Eq. (26), the waves traveling on both paths of the loop are out of phase. On the other hand, the frequencies given by Eq. (27) correspond to the eigenmodes of a loop alone.

In the particular case of a symmetric loop ($d_2=d_3, \Delta L=0$), the transmission coefficient becomes

$$T=\frac{16}{25-9\cos^2(\alpha' d_2)}. \tag{28}$$

In contrast to the case of an asymmetric single loop, the transmission through a symmetric loop never becomes zero.

A great deal of theoretical work has been devoted recently[26,33–35] to the understanding of the relation between the phase of the transmission and the density of states (DOS) depending on whether the system exhibits or not zeroes of transmission. Some of these researchers tried to explain by continuum[33,34] and lattice[35] scattering models the phase jumps observed in a few experiments realized on mesoscopic systems.[11,12] Here, we shall show theoretically and verify experimentally the existence of phase jumps in the transmission of a single loop as far as the constituting wires of the loop have different lengths. In the particular case when the wire lengths become identical, the phase increases monotonically as a function of the frequency. These results are summarized in Fig. 2, where we have plotted the amplitude $\sqrt{T}$ [Figs. 2(a) and 2(d)], the phase [Figs. 2(b) and 2(e)], and the phase time [Figs. 2(c) and 2(f)] for a symmetric (right panel) and an asymmetric (left panel) loop. The lengths of the wires of the asymmetric (symmetric) loop are $d_2=0.355$ m and $d_3=0.655$ m ($d_2=d_3=0.5$ m), whereas the dielectric permittivity is taken to be $\varepsilon=2.3$. The solid curve represents the theoretical results whereas the dotted curve corresponds to the experimental ones. The experiments were performed using standard 50 Ω coaxial cables assembled together with metallic T-shaped connectors. The cross section of the cables is negligible compared to their length and to the propagation wavelength, so that the assumption of monomode propagation is satisfied. The transmission measurements have been realized by using a tracking generator coupled to a spectrum analyzer in the frequency range of 10 to 500 MHz. The attenuation inside the coaxial cables was simulated by introducing a complex relative dielectric permittivity ($\varepsilon=\varepsilon'-j\varepsilon''$). The attenuation coefficient α can be expressed as $\alpha=\varepsilon''\omega/c$. On the other hand, the attenuation specification data supplied by the manufacturer of the coaxial cables in the frequency range of 10 to 500 MHz can be approximately fitted with the expression $\ln\alpha=a+b\ln\omega$, where a and b are two constants. From this fitting procedure, a useful expression for ε'' as a function of frequency can be obtained under $\varepsilon''\simeq 0{,}017 f^{-0,5}$ where the frequency f is expressed in the units of hertz. Three successive minima are seen in the transmission through an asymmetric loop [Fig. 2(a)]. The first and the third ones, obtained for frequencies respectively equal to 193.5 and 387 MHz, respectively, correspond to $m'=1$ and $m'=2$ in Eq. (27). The second minimum at 340.3 MHz is associated with $m=0$ in Eq. (26). The transmission zeroes give rise to abrupt phase change by π in the phase of the transmission function [Fig. 2(b)] or to delta peaks in the transmission phase time [Fig. 2(c)]. It is worth noticing that the phase jump is slightly enlarged and becomes less than π because of the dissipation in the cables.

These results agree with the experiments of Yacoby *et al.*[11] and Schuster *et al.*[12] in which the conductance through a quantum dot shows a phase change by π between each pair of adjacent in-phase resonances. In contrast to Fig. 2(a), Fig. 2(d) clearly shows that the transmission through a symmetric loop does not reach zero and therefore the corresponding phase [Fig. 2(e)] increases monotonically. These results clearly show, in accordance with the theoretical works of Refs. 26, 33–35, that the phase time measurements in a symmetric loop reflect the DOS in this system, whereas in an asymmetric loop these two quantities are different because of the transmission zeroes.

An interesting result that can be deduced from the phase time τ [Figs. 2(e) and 2(f)] is the group velocity[32] v_g

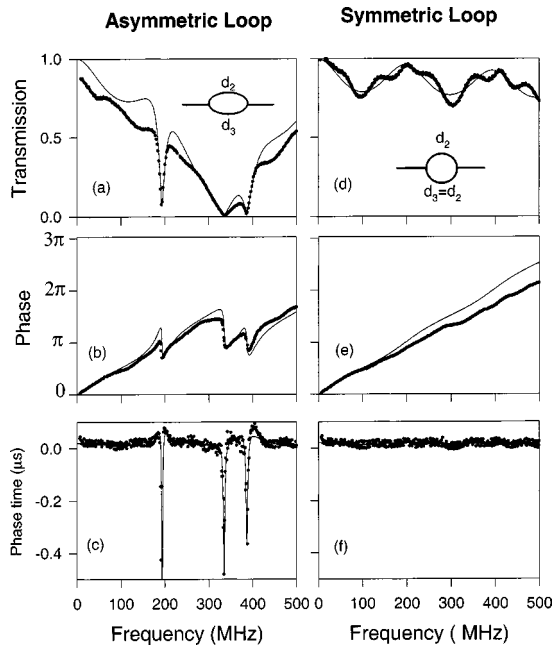

FIG. 2. Transmission coefficient (a) and (d), phase (b) and (e), and phase time (c) and (f) as function of the frequency for an asymmetric single loop ($d_2=0.36$ m and $d_3=0.65$ m) and a symmetric single loop ($d_2=d_3=0.5$ m).

$=(\ell/\tau)$, where ℓ is the total length of the finite structure. In contrast to a symmetric loop, an asymmetric loop may give rise to negative group velocity around the transmission zeroes because of the negative peaks in the phase time spectrum. In the example of Fig. (2c), the value of v_g becomes as small as $-0.05c$ around the peaks situated at 340 and 387 MHz.

The idea of negative group velocity amounts to several decades with the challenge of realizing pulse advancement comparable to pulse width, with a low level of pulse distortion. Indeed, it is well known that inside an absorption line the refractive index (or equivalently the phase of transmission [Fig. 2 (b)]) may take a steep drop,[36] resulting in an anomalous dispersion and consequently a light pulse propagation at a group velocity faster than c or even negative[37,38] in absorbing, homogeneous dielectric materials. More recently,[13,14,39] negative group velocity has been found both theoretically and experimentally in media made of atomic vapor cells in the presence of gain. In all this work, it was clearly pointed out that such superluminal behavior is not at odds with either causality or Einstein's theory of special relativity, but it exclusively results from interference between the different frequency components of the pulse in an anomalous dispersion region.[15] In addition, as argued by several authors,[14,40–42] it is not the group velocity, but rather the front velocity that must be no greater than c. In circuits, a discussion of negative group velocity in a simple bandpass filter[43] clearly demonstrated negative group delays. However, for a filter, the concept of group velocity is not defined. Recently, Munday and Robertson[44] showed experimentally negative group velocity in 1D photonic circuit made of alternating two different impedance coaxial cables. However, from the theoretical point of view,[26,45] it has been shown that for lossless, 1D filter, negative phase time[26] or equivalently negative group velocity[45] are not possible. These results let the authors suppose that the dissipation inside the coaxial cables may be at the origin of the observed negative group velocity. However, other experiments on coaxial cables made of alternating different cables[46] or SLS (see Sec. B) do not show such negative group velocity. On the other hand, the results presented in Fig. 2(e) clearly show both theoretically and experimentally that a single asymmetric loop made of coaxial cables exhibits negative phase time τ around the transmission zeros of the structure. Therefore, we believe that this structure could be a good candidate for obtaining negative group velocity.

In the next section, we shall discuss the bandgap structures as well as the amplitudes and phase times of the transmission when several SLS are connected together periodically by finite segments with or without a defect. A preliminary report of these results on the band structure and transmission spectrum appeared recently[47] for asymmetric SLS.

B. Several loops

Now, we turn to the analytical and experimental results for the transmission of electromagnetic waves through SLS made of several loops. When the media constituting the SLS are made of identical materials (i.e., $\varepsilon_1=\varepsilon_2=\varepsilon_3=\varepsilon_s=\varepsilon_0=\varepsilon$), the dispersion relation [Eq. (10)] can be rewritten in the following simplified form:

$$\xi=\frac{1}{2\sin\left(\frac{\alpha' L}{2}\right)\cos\left(\frac{\alpha'\Delta L}{2}\right)}\left\{\sin(\alpha' d_1)\left[\frac{5}{4}\cos(\alpha' L)-\frac{1}{4}\cos(\alpha'\Delta L)-1\right]+\cos(\alpha' d_1)\sin(\alpha' L)\right\}, \quad (29)$$

where $\Delta L=d_2-d_3$, $L=d_2+d_3$ and $\alpha'=\omega\sqrt{\varepsilon}/c$.

Figure 3 displays the projected band structure; that is, the frequency $\omega/2\pi$ versus ΔL of an infinite SLS for given values of L and d_1: $L=1.06$ and $d_1=0.5$ m, respectively. The shaded areas correspond to frequencies for which $|\xi|<1$ and represent bulk bands. These areas are separated by minigaps. Inside these gaps, the dashed lines show the frequencies for which the denominator of ξ [Eq. (29)] vanishes. The dashed horizontal and curved lines correspond to the vanishing of $\sin(\alpha' L/2)$ and $\cos(\alpha'\Delta L/2)$, respectively.[48] They define the frequencies at which the transmission through a single loop is equal to zero. The existence and width of the minigaps are influenced by both the periodicity of the structure and the zeros of transmission. Let us notice that some of the minigaps having a lozenge pattern display a large variation with ΔL. In the latter minigaps, one can observe the existence of very narrow (almost flat) minibands. These minibands become totally flat (and coincide with the horizontal dashed lines) if L is taken to be equal to 1 m instead of 1.06 m. Indeed, for $L=1$ m, we have $L=2d_1$, and one can easily check that both the numerator and denominator of Eq. (29) vanish simultaneously at the frequencies represented by the dashed lines. The physical meaning of such

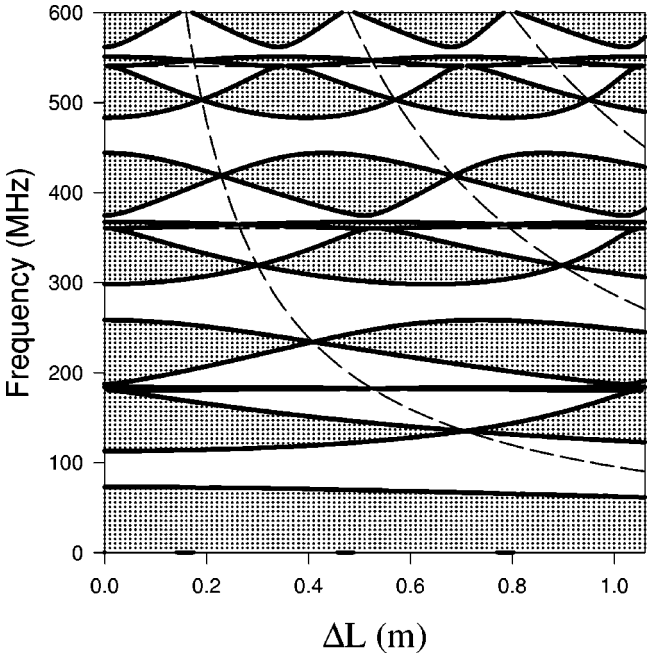

FIG. 3. Projected band structure of the SLS as function of $\Delta L = d_2 - d_3$ for $d_1 = 0.5$ m and $L = d_2 + d_3 = 1.06$ m. The shaded areas represent the bulk bands. The dashed curves indicate the frequencies for which the denominator of ξ [Eq. (29)] vanishes.

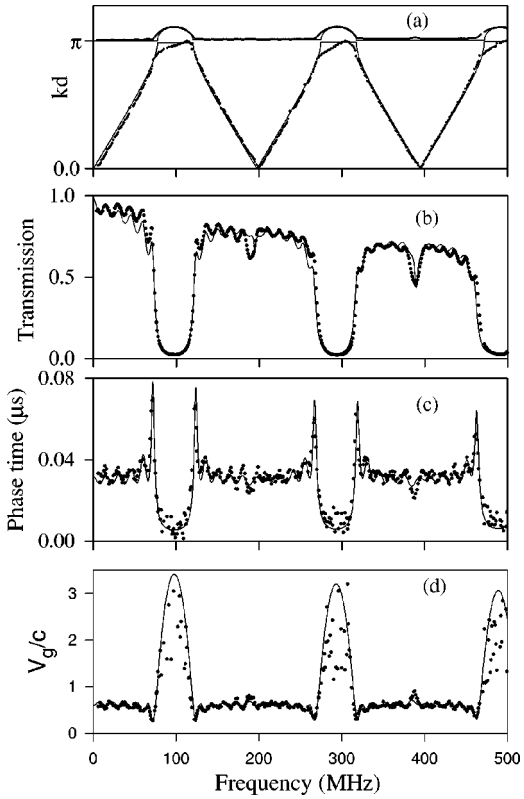

FIG. 4. (a) Theoretical band structure of the infinite symmetric SLS with $d_1 = d_2 = d_3 = 0.5$ m and $\varepsilon = 2.3$. The experimental curve (dots) is obtained from the amplitude (b) and the phase (c) of the transmission through a finite-sized SLS. (b) Theoretical (solid line) and experimental (dots) variations of the transmission coefficient through a nondefective finite SLS containing $N = 6$ loops with the same characteristic lengths as in (a). (c) Theoretical (solid line) and experimental (dots) variations of the phase time in the same conditions as in (b). Theoretical (solid line) and experimental (dots) variations of the group velocity in the same conditions as in (b) and (c).

flat bands is that the infinite structure possesses localized states at these frequencies, while the transmission through the finite structure remains equal to zero. One also observes in Fig. 3 that, at certain values of ΔL (for instance, $\Delta L \sim 0.25$ m), one can obtain a series of narrow minibands separated by large gaps. This results from the fact that the points where the minibands close, align more or less vertically in such a way that a few successive bands may become very narrow.

In what follows, we shall detail the results concerning the case of symmetric SLS ($d_2 = d_3$) and then give some results about the case of an asymmetric SLS ($d_2 \neq d_3$). We also show at the end of this section that the width of the bandgaps may be enlarged by coupling several SLS of different physical characteristics.

1. Symmetric SLS

First, we analyze the properties of the band structure and the transmission for a perfect SLS, without defect. Figure 4(a) shows the first five dispersion curves (full lines) in the band structure of an infinite serial loop waveguide ($N \to \infty$) with the same characteristic lengths ($d_1 = d_2 = d_3 = 0.5$ m). One can observe a gap after the first passband and another gap between the third and the fourth bands. The gaps between the second and the third bands and between the fourth and the fifth bands (situated at $kd = 0$) close. The real and imaginary parts of the reduced wave vector kd are in very good agreement with the experimental results (dotted curves) obtained from the amplitude $|t|$ [Fig. 4(b)] and the phase Φ [Fig. 4(c)] of the transmission through a finite sized SLS. Indeed, writing the transmission coefficient $t_r = |t| e^{j\Phi}$ under the form $t_r = e^{jk\ell}$, where ℓ is the total length of the finite structure, one obtains the effective wave number

$$k = \frac{\Phi}{\ell} - j\frac{ln|t|}{\ell}. \tag{30}$$

One can note that despite the small number of serial loops ($N = 6$) used in the finite structure, the amplitude and the phase describe very well the band structure of the infinite system $N \to \infty$ [Fig. 4(a)]. The attenuation effect in coaxial cables induces a transmission depletion particularly at high frequencies. As mentioned earlier, the phase time in a symmetric SLS is equivalent to the DOS;[26,33,34] therefore, Fig. 4(c) is also an illustration of the DOS in these 1D photonic crystals. A large enhancement of the DOS is observed in the vicinity of the band edges. The number of oscillations in each band (that is related to the number of loops in the finite structure) gives the number of states. The behavior of the group velocity[32] $v_g = (\ell/\tau)$ is given in Fig. 4(d). For a 1D PBG, v_g is equivalent to the inverse of the DOS. It is well known that in infinite 1D systems, the density of modes approaches infinity at the band edge and the group velocity becomes very small. In a finite system, however, the electromagnetic mode density is an oscillating function rather than a monotonous function [Fig. 4(c)]. The enhancement of the

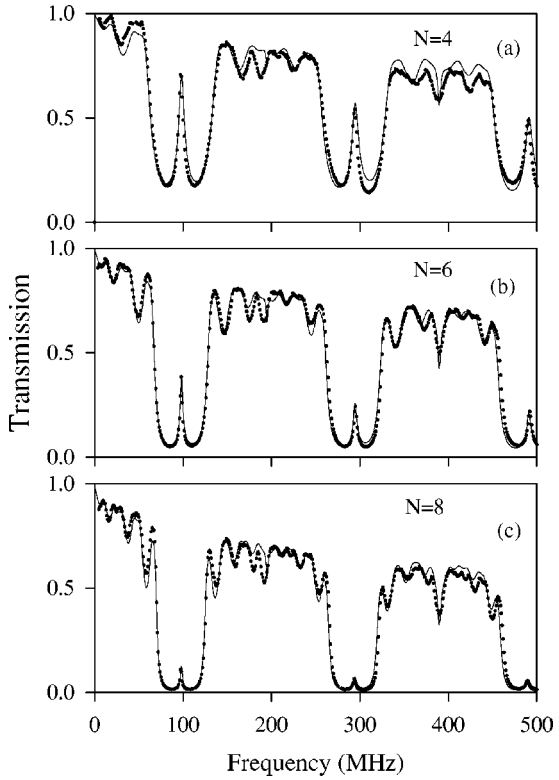

FIG. 5. Theoretical (solid line) and experimental (dots) variations of the transmission coefficient through a finite SLS of N loops containing a defect of length $d_0=1$ m located in the middle of the SLS (cell p) ($d_1=d_2=d_3=0.5$ m and $\varepsilon=2.3$). (a) $N=4$ and $p=3$, (b) $N=6$ and $p=4$, and (c) $N=8$ and $p=5$.

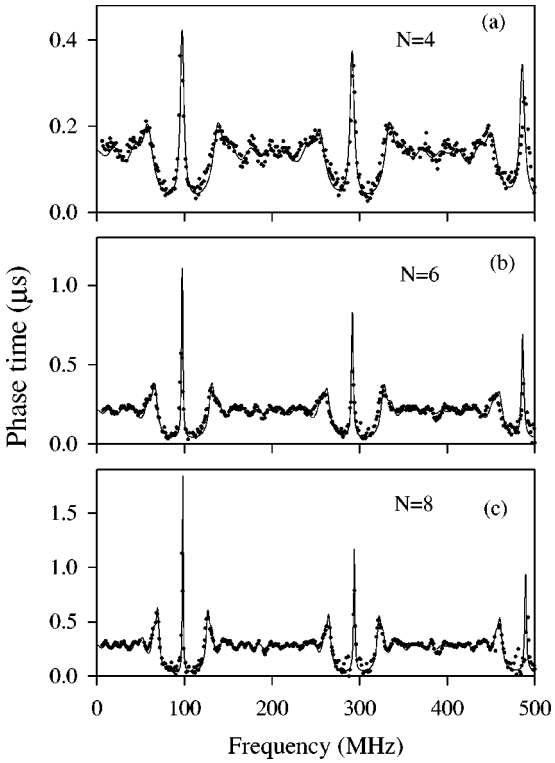

FIG. 6. Theoretical (solid line) and experimental (dots) variations of the phase time as function of the frequency. The parameters are the same as in Fig. 5.

phase time (or the DOS) at the band edges induces a small group velocity [Fig. 4(d)] which has been shown to be of potential interest in application to band-edge lasing and optical delay lines.[49] In addition, one can notice inside the passbands, the group velocity is equal to $0.66c$. However, inside the gaps, anomalous dispersion occurs and superluminal velocities are expected such that $3c \leqslant v_g \leqslant 3.5c$. These results are in accordance with those of Haché and Poirier.[17,50] The system studied here presents an advantage: all the segments in the periodic structure are made of the same material instead of being constructed by two different materials.

Now, we study the transmission spectrum and the phase time through the structure when a segment of length $d_1=0.5$ m is replaced by a defect branch of length $d_0=1$ m in the middle of the SLS waveguide. The results are presented in Fig. 5 for three different values of N. First, one can notice that by increasing N, the transmission decreases more rapidly to zero at the band edges [Fig. 5(c)]. The effect of the defect branch is to induce defect (or localized) modes in the forbidden bands. The frequencies of these modes are almost independent of N, whereas their intensities decrease progressively with increasing N (Fig. 5). This decrease of the intensities may appear to be in contradiction with the fact that, by increasing N, the localization degree of these modes around the defect increases and therefore the peaks associated with the defect modes narrow. However, this behavior can be explained by the dissipation inside the coaxial cables that lead to a widening of the peaks due to the absorption phenomenon, but also to a decrease in the transmitted intensity due to an enhancement of the reflected intensity.

The evolution of the phase time versus the frequency is depicted in Fig. 6 for the same values of N as in Fig. 5. In contrast to the amplitude of the localized states in the transmission spectra of Fig. (5), the phase time associated with the defect modes increases with increasing N. Indeed, the intensity of the peaks in the phase time is related to the lifetime of the resonances and it reflects the time spent by the photon inside the defect (cavity) before its transmission.[51] Therefore, when N increases, the defect modes become more localized and the trapping time of photons increases. These results indicate that the characterization of localized modes in SLSs, in which the attenuation is not negligible, is easier with phase time analysis than with amplitude measurements. To give a better insight into the localization properties of photons inside the defect segment, Fig. 7 displays the phase time of the defect mode lying in the first gap of Fig. 6 for different values of N. One can notice that the lifetime of the resonances associated with the defect mode increases from 0.42 to 1.1 μs when N increases from $N=4$ to $N=8$ [Fig. 7(a)]. The integration of the phase time [Fig. 7(b)] shows a monotonic rise by almost π (one state) near the maximum of the resonance. Finally, an analysis of the local DOS [Fig. 7(c)] as function of the space position x clearly shows that the defect mode is localized in the defect segment and rapidly decays in the vicinity of the defect. However, the localization is more pronounced when the SLS size is larger. These results indicate that most of the time spent by the

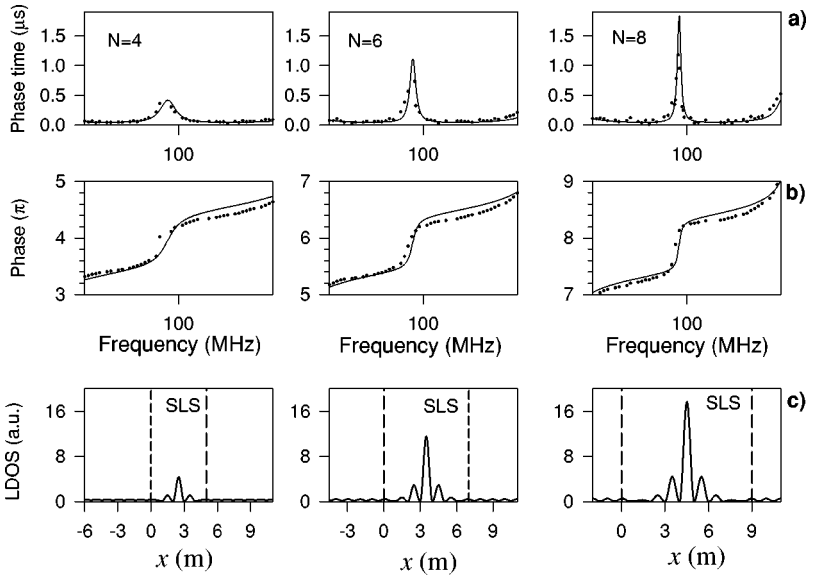

FIG. 7. Theoretical (solid line) and experimental (dots) variations of the phase time (a) and the phase (b) of the localized mode in the first gap of Fig. 6. Variation of the local density of states (DOS) as function of the space position x for the localized modes in (a) and (b).

photon during the transmission process was inside the defect segment. Indeed, once a photon enters the defect region, it encounters two Bragg reflectors (the periodic parts) around it. Since the frequency of the photon is in the gap of the Bragg reflectors, the photon will be strongly reflected back to the defect region. The defect region, acts as a Fabry–Perot cavity and the photon can not escape from this region. The long time spent in the defect region results in very high energy density around the defect.[32]

When the defect is inserted far from the middle of the SLS, the amplitude of the localized modes decreases progressively. This effect is depicted in Fig. 8 for $N=6$. Indeed, the amplitude of the defect mode decreases when the defect lies between the second and the third loops [Fig. 8(b)], and practically vanishes when the defect branch is inserted between the first and the second loops [Fig. 8(c)]. One can notice the same behavior when the defect is located between the fourth and the fifth loops and between the fifth and the sixth loops, respectively, because of the perfect symmetry of the SLS. These behaviors may be explained qualitatively as follows: when the defect is inserted in the middle of the SLS, the SLS behaves as two identical waveguides with N/2 loops connected with a defect. Because of the symmetry of the system, constructive interferences occur that lead to the enhancement of the amplitude of the transmission. However, when the defect branch lies far from the middle of the SLS, the SLS behaves as two linked waveguides with different number of loops (2, 4 or 1, 5). Each of the linked waveguides contributes in its own way to the transmission of the SLS. Thus, destructive effects are responsible for the decrease in amplitude when the defect is moved away from the middle of the SLS. This qualitative interpretation agrees with the evolution of the phase time corresponding to defect modes which decreases also when the defect is inserted far from the middle of the SLS (Fig. 9).

On the other hand, the transmission inside the passbands is also affected by the presence of the defect. Indeed, the amplitude of the oscillations in the passbands is greater in the perturbed SLS (Figs. 5 and 8) than in the perfect one (Fig. 4) because one state (defect mode) is now detached from the bulk band (see subsequent discussion). This behavior is particularly important when the defect is located far from the middle of the SLS [Figs. 8(b) and 8(c)]. In these cases, the amplitude of the oscillations in the passbands exhibits strong variations due to destructive effects.

The comparison of Figs. (5) and (8) shows that the frequency of the defect mode does not depend on the defect location in the SLS; however, the frequencies are very sen-

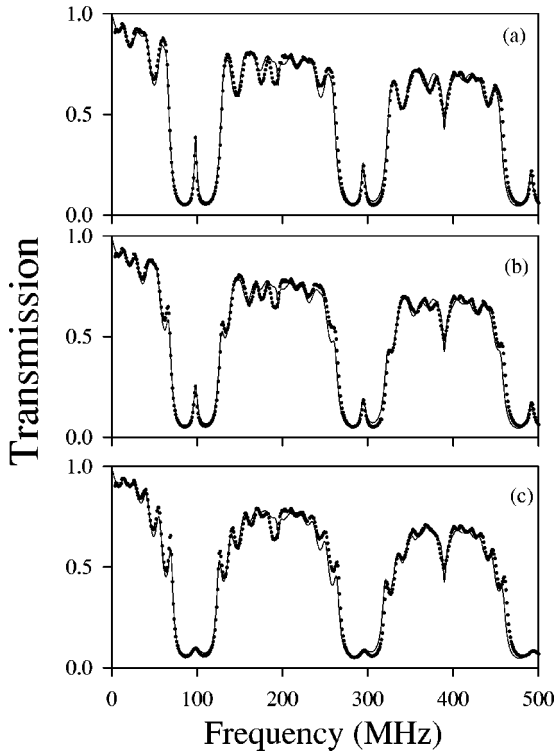

FIG. 8. Theoretical (solid line) and experimental (dots) variations of the transmission coefficient through a finite SLS of six loops containing a defect of length $d_0=1$ m located in the cell p ($d_1=d_2=d_3=0.5$ m and $\varepsilon=2.3$). (a) $p=4$, (b) $p=3$, and (c) $p=2$.

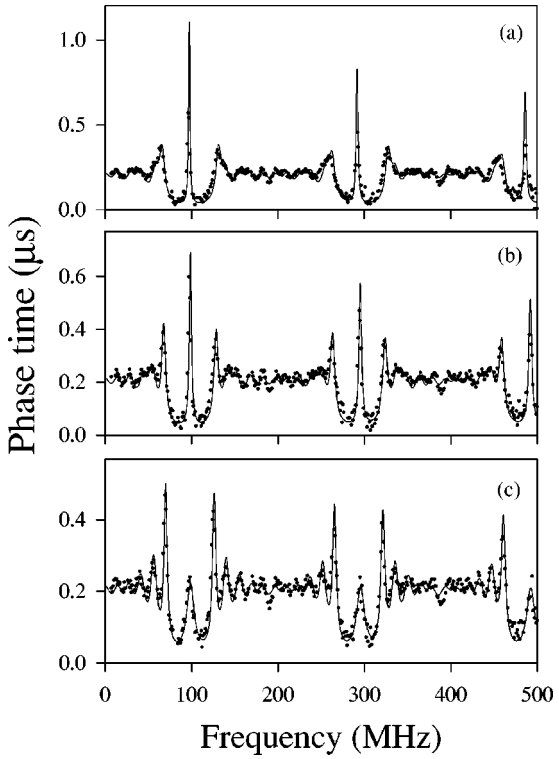

FIG. 9. Theoretical (solid line) and experimental (dots) variations of the phase time as function of the frequency. The parameters are the same as in Fig. 8.

sitive to the defect length d_0, as is shown in Fig. 10. The hatched areas correspond to the bulk bands. The solid lines represent the computed frequencies in an infinite SLS with a defect segment whereas the dots correspond to the experimental measurements. The localized modes emerge from the bulk band, decrease in frequency when d_0 increases and finally merge into a lower bulk band. At each frequency, there is a periodic repetition of the localized states as function of d_0. One notes the overall good agreement between the experimental measurements and the theoretical results.

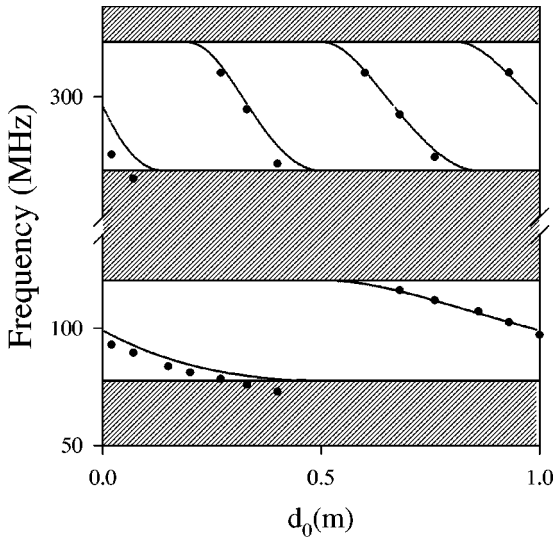

FIG. 10. Comparison between theoretical and experimental frequencies of the localized states associated with the presence of a defect branch of length d_0, inserted in the cell p of a SLS. Solid lines: calculated frequencies in an infinite SLS ($N\rightarrow\infty$); dots: measured frequencies in a finite SLS with $N=6$ and $p=4$. The other parameters are $d_1=d_2=d_3=0.5$ m and $\varepsilon=2.3$. The dashed areas correspond to the bulk bands.

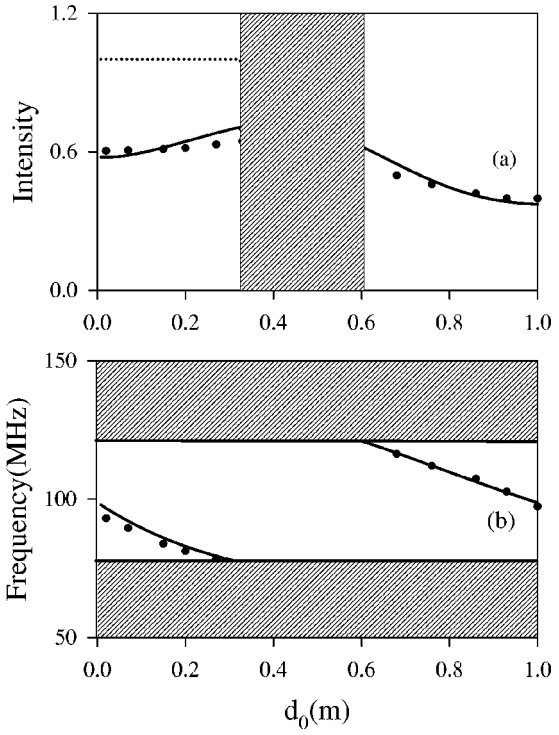

FIG. 11. (a) Variation of the intensity of the transmitted localized mode located in the first gap as function of the defect length d_0. The defect is inserted in the middle of a SLS with $N=6$ and $p=4$. Dashed lines: calculated intensities when the dissipation effect is neglected. Solid lines: calculated intensities when the dissipation is taken into account. The dots represent the measured intensities. The shaded areas correspond to the frequency region when localized modes merge inside the bulk bands [(b)]. The other parameters are $d_1=d_2=d_3=0.5$ m and $\varepsilon=2.3$. (b) The same as in Fig. 10.

We have also studied the evolution of the power transmission at the frequency of the defect mode falling in the first gap as a function of the defect length d_0. Figure 11(a) illustrates this evolution in the case of a defect inserted in the middle of a SLS constructed of $N=6$ loops. Let us recall that the power transmission is stronger when the defect is inserted closer to the middle of the waveguide (see Figs. 8 and 9). The hatched area in Fig. 11(a) corresponds to the situation in which the defect mode merges into a bulk band [Fig. 11(b)]. The dashed line in Fig. 11(a) represents the computed intensity when dissipation inside the cables is neglected. One can notice that the transmission is unity for all frequencies, this property is commonly verified in any symmetric composite system, whereas it may only happen under special conditions if the composite media is not symmetric. The full line corresponds to the computed intensity when dissipation is taken into account. The transmission, which is now smaller than unity, increases progressively with the defect length until the localized mode merges with the first bulk band. With increasing d_0, a defect mode emerges from the second bulk band, its intensity decreases, and reaches a stationary value. In Fig. 11(a), the dots represent the experimental measurements whose evolution is in good agreement with

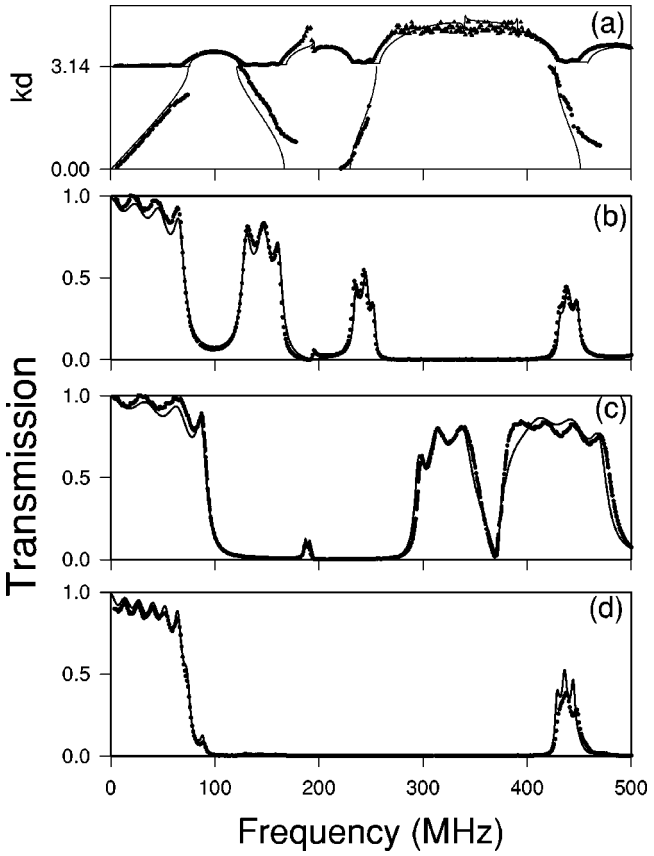

FIG. 12. (a) Theoretical band structure of the infinite asymmetric SLS with $d_1=0.5$ m, $d_2=0.65$ m, and $d_3=0.36$ m (i.e., $\Delta L=0.29$ m). The experimental curve (dots) is obtained from the amplitude (b) and the phase (not shown) of the transmission through a finite-sized SLS. (b) Theoretical (solid line) and experimental (dots) variations of the transmission coefficient through a finite SLS containing $N=4$ loops with the same characteristic lengths as in (a). (c) The same as in (b), but for $L=0.5$ m and $\Delta L=0.5$ m (i.e., $d_2=0.5$ m and $d_3\simeq 0$.). (d) The same as in (b) and (c), but for a tandem built of the (b) and (c) structures.

the computed results. Fig. 11(b), recalls the frequency of the localized mode as a function of d_0 as well as the location of the bulk bands of the perfect infinite SLS.

2. Asymmetric SLS

An example of the dispersion curve in an infinite asymmetric SLS is depicted in Fig. 12(a) (full lines) for $\Delta L=d_2-d_3=0.29$ m and $L=1$ m. These curves are in good agreement with experimental measurements (dotted curves) obtained from the amplitude [Fig. 12(b)] and the phase (not shown) of the transmission through a finite-sized SLS made of $N=4$ loops. In comparison with symmetric SLS [Fig. 4(a)], asymmetric SLS may exhibit larger gaps [Figs. 12(a) and 12(b)]. The width of the bandgaps discussed earlier may be enlarged by associating in tandem two or several successive SLSs that differ by their physical characteristics. An example of this association is shown in Figs. 12(b) and 12(c) for two different asymmetric SLSs: (i) a SLS with $\Delta L=0.29$ m and $L=1$ m (i.e., $d_2=0.65$ m and $d_3=0.36$ m) [Fig. 12(b)] and (ii) a SLS with $\Delta L=L\simeq 0.5$ m (i.e., $d_2=0.5$ m and $d_3\simeq 0$) [Fig. 12(c)]. In these two cases $d_1=0.5$ m. Figure 12(c) exhibits a large gap at frequencies

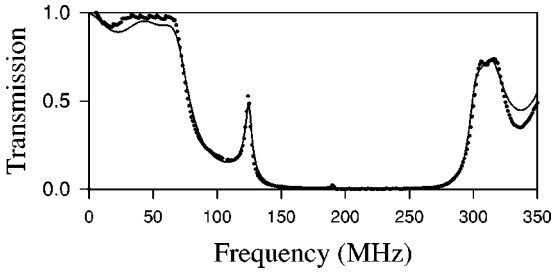

FIG. 13. The same as in Fig. 12(b), but with a defect segment of length $d_f=0.13$ m in the middle of the structure.

lower than in Fig. 12(b); that is, between 100 and 300 MHz. The small feature appearing in the transmission spectrum around 180 MHz inside the large gap is associated with a flat band. It occurs because the actual length ΔL of the loops is slightly different from 0.5 m and the corresponding bands have a small width instead of being totally flat (see also Fig. 3 and the corresponding discussion). Now, by associating in tandem the serial loop structures [Figs. 12(b) and 12(c)], one obtains [Fig. 12(d)] an ultrawide gap in which the transmission vanishes over a large range of frequencies from 80 to 420 MHz. In this structure, the huge gap results from the superposition of the forbidden bands of the individual SLS [Figs. 12(b) and 12(c)]. Theoretical and experimental results are in agreement within the limits of experimental precision.

If a defect is included in the structure, a localized state can be created in the gap. A defect in a SLS can be realized by replacing a finite wire of length d_1 by a segment of length $d_f\neq d_1$ in one cell of the waveguide. The measured transmission spectrum for the structure depicted in Fig. 12(c) with a defect segment of length $d_f=0.13$ m in the middle of this structure is shown by the dotted line in Fig. (13). The theoretical transmission is illustrated by the solid line. The measured values are in remarkable agreement with theory. Let us emphasize that the frequency of the defect mode inside the gap depends on the length of the defect segment, whereas the intensity of the peak in the transmission spectrum depends on the number N of loops in the SLS and the location of the defect segment.

V. SUMMARY AND CONCLUSIONS

In this article, we have considered quasi-1D serial loop structures exhibiting very large photonic band gaps (PBGs). Compared to other 1D systems such as star-waveguides, the observed gaps in SLS are significantly larger. The theoretical model assumed the cross sections of the waveguide and of the loops small compared to their linear dimensions. This ensures monomode propagation of the electromagnetic waves. These serial loop structures may present large stop bands and are good candidates for PBG materials. Although they are limited to one dimension and are void of polarization effects, their properties are also described by Maxwell's equations, and some linear[16,52] and nonlinear[50] properties similar to those encountered in optical PBG materials have been reported. The measurements of the amplitude and the phase of the transmission coefficients through the finite-sized SLS enables us to deduce several properties on the wave

propagation through such structures as dispersion curves, phase times, and therefore DOSs as well as group velocities.

In addition, we have shown that the presence of defect branches in the SLS gives rise to localized states inside the gaps. These defect modes appear as very narrow peaks of strong amplitude in the transmission and the phase time spectra. The localized states are very sensitive to the length of the defects, and to their position in the SLS. The phase time measurements in the SLS are in general different from the DOS, except for the symmetrical SLS, in which these two quantities are equivalent. The experimental results are very well fitted by the 1D theoretical model using the Green's function method.

Let us also stress that, in star waveguides, an important difficulty lies in the technical realization of the boundary condition at the free ends of the resonators, whereas this problem is avoided in SLS.

In this study, the lengths of the finite wires are of the order of the meter and the gaps occur in the hyperfrequency range. However, our theoretical model is in principle universal and is thus also valid in other frequency domains of the electromagnetic spectrum. For example, designing SLS working at optical frequencies requires characteristic lengths d_1, d_2, and d_3 of the order of the micrometer. The manufacturing of such waveguides could be very useful once the problem of radiative and scattering losses is overcome by amplification technique in making, for instance, filtering or multiplexing devices. It would even be more interesting for integrated structures working at optical frequencies. Recent work shows clearly that the manufacturing of such serial loop structures at a submicrometric scale becomes realizable with recent technological developments using high-resolution electron-beam lithography.[53] Nevertheless, the lateral size of such wires is in general of the same order of magnitude as the optical wavelengths, and a more thorough analysis of the scattering processes at the junctions would become desirable. Such a numerical modeling of our SLS is now underway.

ACKNOWLEDGMENTS

One of us (E. E.) gratefully acknowledges the hospitality of the UFR de Physique, Université de Lille I. The authors acknowledge ''Le Fond Européen de Développement Régional'' (FEDER) and ''Le Conseil Régional Nord-Pas de Calais'' for their support.

[1] E. Yablonovitch, Phys. Rev. Lett. **58**, 2059 (1987).
[2] S. John, Phys. Rev. Lett. **58**, 2486 (1987).
[3] J. Martorell and N. M. Lawandy, Phys. Rev. Lett. **65**, 1877 (1990).
[4] E. Yablonovitch, J. Opt. Soc. Am. B **10**, 283 (1993).
[5] See for example: J. D. Joannopoulos, R. D. Meade, and J. N. Winn, *Photonic Crystals* (Princeton University Press, Princeton, 1995); *Photonic Band Gaps and Localization*, edited by C. M. Soukoulis (Plenum, New York, 1993); *Photonic Band Gap Materials*, edited by C. M. Soukoulis (Kluwer, Dordrecht, 1996).
[6] J. D. Joannopoulos, P. R. Villeneuve, and S. Fan, Solid State Commun. **102**, 165 (1997), and references therein.
[7] L. Dobrzynski, A. Akjouj, B. Djafari-Rouhani, J. O. Vasseur, and J. Zemmouri, Phys. Rev. B **57**, R9388 (1998).
[8] J. O. Vasseur, B. Djafari-Rouhani, L. Dobrzynski, A. Akjouj, and J. Zemmouri, Phys. Rev. B **49**, 13446 (1999).
[9] S. Foresi, P. R. Villeneuve, J. Ferrera, E. R. Thoen, G. Steinmeyer, S. Fan, J. D. Joannopoulos, L. C. Kimerling, H. I. Smith, and E. P. Ippen, Nature (London) **390**, 143 (1997).
[10] Z. Q. Zhang, C. C. Wong, K. K. Fung, Y. L. Ho, W. L. Chan, S. C. Kan, T. L. Chan, and N. Cheung, Phys. Rev. Lett. **81**, 5540 (1998).
[11] A. Yacoby, M. Heiblum, D. Mahalu, and M. Shtrikman, Phys. Rev. Lett. **74**, 4047 (1995).
[12] R. Schuster, E. Buks, M. Heiblum, D. Mahalu, V. Umansky, and H. Shtrikman, Nature (London) **385**, 417 (1997).
[13] L. J. Wang, A. Kusmich, and A. Dogarin, Nature (London) **406**, 277 (2000).
[14] A. Dogarin, A. Kusmich, and L. J. Wang, Phys. Rev. A **63**, 053806 (2001).
[15] B. Macke and B. Segard, Eur. Phys. J. D **23**, 125 (2003).
[16] G. J. Schneider, S. Hanna, J. L. Davis, and G. H. Watson, J. Appl. Phys. **90**, 2642 (2001).
[17] A. Haché and L. Poirier, Phys. Rev. E **65**, 036608 (2002).
[18] L. Dobrzynski, Surf. Sci. Rep. **11**, 139 (1990).
[19] L. Dobrzynski, J. Mendialdua, A. Rodriguez, S. Bolibo, and M. More, J. Phys. (France) **50**, 2563 (1989).
[20] M. L. Bah, Ph.D. thesis, University of Lille I, 1995.
[21] A. Mir, PhD thesis, University of Meknés, Morocco, 2002.
[22] M. Buttiker and R. Landauer, Phys. Rev. Lett. **49**, 1739 (1982).
[23] M. Buttiker, Phys. Rev. B **27**, 6178 (1983).
[24] E. H. Hauge and J. A. Stovneng, Rev. Mod. Phys. **61**, 917 (1989).
[25] V. Laude and P. Tournois, J. Opt. Soc. Am. B **16**, 194 (1999).
[26] M. L. H. Lahlaouti, A. Akjouj, B. Djafari-Rouhani, L. Dobrzynski, M. Hammouchi, E. H. El Boudouti, A. Nougaoui, and B. Kharbouch, Phys. Rev. B **63**, 035312 (2001).
[27] M. L. Bah, A. Akjouj, E. H. El Boudouti, B. Djafari-Rouhani, and L. Dobrzynski, J. Phys.: Condens. Matter **8**, 4171 (1996).
[28] P. Yeh, *Optical Waves in Layered Media* (Wiley, New York, 1988).
[29] R. P. Stanley, R. Houdré, U. Oesterle, M. Ilegems, and C. Weisbuch, Phys. Rev. A **48**, 2246 (1993).
[30] R. Wang, J. Dong, and D. Y. Xing, Phys. Status Solidi B **200**, 529 (1997).
[31] M. Sigalas, C. M. Soukoulis, E. N. Economou, C. T. Chan, and K. M. Ho, Phys. Rev. B **48**, 14121 (1993).
[32] S. Zhu, N. Liu, H. Zheng, and H. Chen, Opt. Commun. B **174**, 139 (2000).
[33] H.-W. Lee, Phys. Rev. Lett. **82**, 2358 (1999).
[34] T. Taniguchi and M. Buttiker, Phys. Rev. B **60**, 13814 (1999), and references therein.
[35] A. Levy Yeyati and M. Buttiker, Phys. Rev. B **62**, 7307 (2000).
[36] L. Brillouin, *Wave Propagation and Group Velocity* (Academic, New York, 1960).
[37] S. G. B. Garret and D. E. McCumber, Phys. Rev. A **1**, 305 (1970).
[38] S. Chu and S. Wong, Phys. Rev. Lett. **48**, 738 (1982).
[39] A. M. Steinberg and R. Chiao, Phys. Rev. A **49**, 2071 (1994).
[40] P. C. Peters, Am. J. Phys. **56**, 129 (1988).
[41] R. Landauer and T. Martin, Rev. Mod. Phys. **66**, 217 (1994).
[42] G. Diener, Phys. Lett. A **223**, 327 (1996).
[43] M. W. Mitchell and R. Y. Chiao, Am. J. Phys. **66**, 14 (1998).
[44] J. N. Munday and W. M. Robertson, Appl. Phys. Lett. **81**, 2127 (2002).
[45] G. D. D'Aguanno, M. Centini, M. Scolara, C. Sibilia, M. Bloemer, C. M. Bowden, J. M. Haus, and M. Bertolotti, Phys. Rev. E **63**, 036610 (2001).
[46] A. Haché and L. Poirier, Appl. Phys. Lett. **80**, 518 (2002).
[47] A. Mir, A. Akjouj, J. O. Vasseur, B. Djafari-Rouhani, N. Fettouhi, E. H. El Boudouti, L. Dobrzynski, and J. Zemmouri, J. Phys.: Condens. Matter **15**, 1593 (2003).
[48] J.-B. Xia, Phys. Rev. B **45**, 3593 (1992).
[49] M. D. Tocci, M. Scalora, M. J. Bloemer, J. P. Dowling, and C. Bowden, Phys. Rev. A **53**, 2799 (1996).
[50] L. Poirier and A. Haché, Appl. Phys. Lett. **78**, 2626 (2001).
[51] M. Beyindir and E. Ozbay, Phys. Rev. B **62**, R2247 (2000).
[52] R. D. Pradhan and G. H. Watson, Phys. Rev. B **60**, 2410 (1999).
[53] J. V. Hryniewicz, P. P. Absil, B. E. Little, R. A. Wilson, and P. T. Ho, IEEE Photonics Technol. Lett. **12**, 320 (2000).